ELSEVIER

Global and Planetary Change 11 (1995) 127–138

GLOBAL AND PLANETARY CHANGE

Records of climatic change in the Canadian Arctic: towards calibrating oxygen isotope data with geothermal data

Hugo Beltrami [a,*], Alan E. Taylor [b]

[a] Department of Earth and Planetary Sciences and Centre for Climate and Global Change Research, McGill University, 3450 University Street, Montréal, Québec H3A 2A7 Canada

[b] Terrain Sciences Division, Geological Survey of Canada, 601 Booth Street Ottawa, Ontario K1A 0E8 Canada

Accepted 10 July 1995

Abstract

Borehole temperature–depth data have been combined with oxygen isotope data from an ice core at a nearby location in the Canadian Arctic to calibrate the oxygen isotope data to ground temperature histories. The relationship of oxygen isotope data to ground surface temperature history is $\delta^{18}O = 0.42\,\Delta T_g$ and this reproduces the main features of the observed subsurface temperature profile measured at the borehole site. These results suggests that oxygen isotope data are a good representation of the regional, long term climatic variations at these latitudes. Discrepancies between the observed subsurface profile and the theoretical profile calculated from the calibrated oxygen isotope time series may be explained in terms of the different character of the records, in particular snow cover, and active layer processes.

1. Introduction

It is now well established that ground temperature histories (GTHs) can be determined from the analysis of temperature perturbations measured in boreholes. For reviews see Pollack and Chapman (1993), Vasseur and Mareschal (1993) and Beltrami and Chapman (1994). Several analyses of geothermal data have revealed a marked warming in the last century. However, the warming inferred is not homogeneous but displays a spatial variability consistent with the predictions of GCMs for increased concentrations of atmospheric carbon dioxide. For example, the warming during the last 100 years inferred in Alaska is between 2–4°C (Lachenbruch and Marshall, 1986), 1–2°C in eastern and central Canada (Beltrami and Mareschal, 1991; Beltrami and Mareschal, 1992; Beltrami and Mareschal, 1993; Beltrami et al., 1992; Shen and Beck, 1992; Wang et al., 1992), and less than 1°C in Utah (Chisholm and Chapman, 1992; Harris and Chapman, 1995). About half of the inferred warming for this century in eastern Canada appears to be due to the recovery from a colder period which may be associated with the Little Ice Age, also documented from geothermal data.

In all the above analyses, the inferred temperatures appear to be robust and independent of the model and inversion procedure used to interpret the subsurface climatic signal. Reconstructed GTHs

* Present address: Department of Geology, St. Francis Xavier University, P.O. Box 5000, Antigonish N.S., B2G-2W5, Canada. e-mail: hugo@pooh.geophys.mcgill.ca http://www.eps.mcgill.ca/~hugo/index.html.

SSDI 0921-8181(95)00006-2

have, however, limited resolution. Studies of the resolution of past climatic events from geothermal data (Clow, 1992; Beltrami and Mareschal, 1995) have shown that the estimated model parameters are obtained as averages over at least 60% of the time centered on an event. That is, the signal recovered by inversion for climatic events centered 100 years before present (aBP) would be spread over 60 years, and for an event which occurred 500 aBP, it would appear stretched over 300 years. This relation between time and the temporal spread of the recovered signal varies linearly with the time of occurrence, although it is not temporally symmetric.

Thus, GTHs from geothermal data provide a good estimate of the integrated ground surface temperature changes, but with a resolution that decreases rapidly with time as a result of the diffusive character of the heat conduction process. Proxy records, on the other hand, have higher resolution but their interpretation as a climatic indicator is not always straightforward. For oxygen isotope data from ice cores, for instance, this arises from the complicated processes involved in precipitation in the Arctic regions (e.g. Charles et al., 1994).

Oxygen isotope ratios measured in ice cores are interpreted as representing average air temperature conditions at a given time (Charles et al., 1994; Bradley, 1985) but also reflect changes in both water vapour history and snow surface processes (Thompson et al., 1986). In addition, these records represent mainly summer atmospheric conditions, since the bulk of precipitation in high latitude regions falls in summer. Recent work (Grootes and Steig, 1992) has shown that $\delta^{18}O$ represents accurately the temperature at the time of precipitation, but may not represent climatic conditions on average; i.e., it does not snow all the time, but in discrete events, and the coldest events might not be recorded in the oxygen-isotope record. Furthermore, wind scouring can affect the snow accumulation regime, resulting in a wide range of "climatic" inferences from ice cores in slightly different, but nearby, places; such records require a detailed study of present and past wind patterns to implement appropriate corrections to the

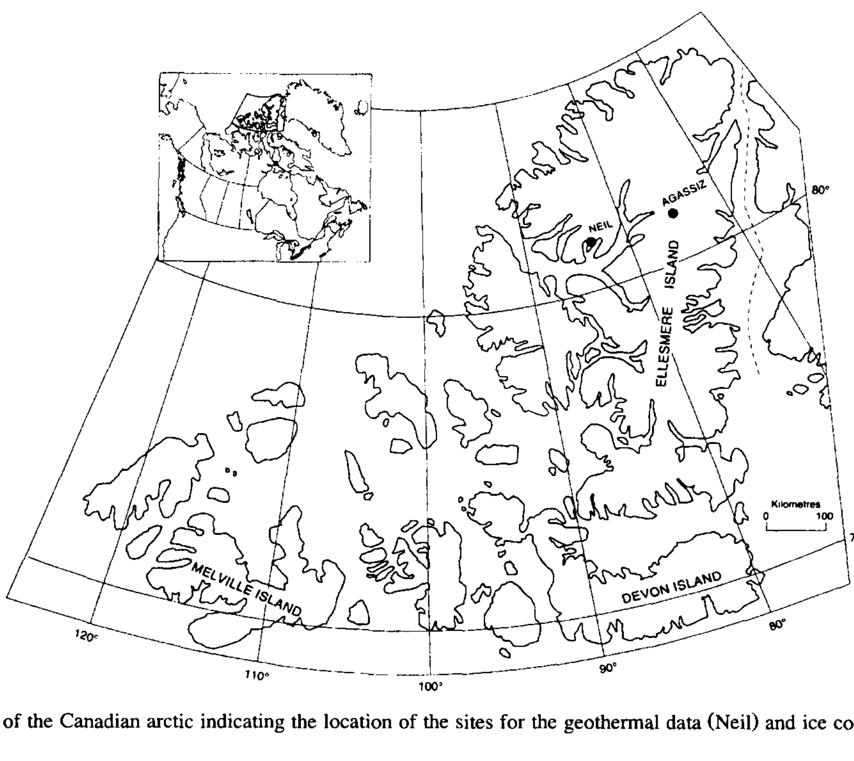

Fig. 1. Map of part of the Canadian arctic indicating the location of the sites for the geothermal data (Neil) and ice core (Agassiz) analyzed in this study.

$\delta^{18}O$ record (e.g. Fisher et al., 1983; Fisher and Koerner, 1994).

In this work, we use a straightforward method for combining geothermal data with high resolution proxy data, in this case oxygen isotope data from the Agassiz ice cap in the Canadian Arctic (Fig. 1; Fisher et al., 1983) to reconstruct ground temperature histories with higher resolution than those obtained from geothermal data alone, or in other words to calibrate oxygen isotope data with geothermal data. We show that the high resolution GTH resulting from the combination of geothermal and oxygen isotope data, when used as a boundary condition at the Earth's surface adequately reproduces the observed subsurface temperature perturbation at a location nearby.

Another approach has been to calibrate oxygen isotope data and air temperature using temperature–depth profiles in ice cores (Cuffey et al., 1992, 1994). This, however, involves the dynamics of ice in the form of a rather complex model and its application to the Agassiz ice cap would be dependent on the ice model boundary conditions.

2. Data

2.1. Geothermal data

The Neil well (80°44.6′ N, 83°4.8′ W; Fig. 1) lies at an elevation of 497 m above sea level, near the center of a peninsula about 9 km wide, some 180 km W of the Agassiz '79 borehole. The topographic relief of the peninsula may have an effect on the ground temperatures, but the magnitude depends on the lapse rate in air and is small. Temperature data to 1980 are published in Taylor et al. (1982) but several additional logs were taken subsequently. We used a detailed temperature log measured in 1991 (Fig. 2a), some 17 years following drilling, and assured ourselves that there was no residual curvature in the temperature–depth profiles attributable to the drilling.

Over the depth section considered at the Neil well, sandstones and siltstones predominate (70%) but are interbedded with shale (27%) and other lithologies (Fig. 2d) Representative thermal conductivity measurements at approximately 30 m intervals (Fig. 2c) were made by the divided bar technique using chip samples recovered during the drilling procedure (Sass et al., 1971; Jessop, 1990, Ch. 2.9).

2.2. Oxygen isotope data

The Agassiz 1979 ice borehole (80°49.2′ N, 72°53.8′ W; Fig. 1), lies at an elevation of 1700 m above sea level. We use the 25-year averages of the $\delta^{18}O$ record for the past 2000 years (Fig. 3; Fisher et al., 1983).

The dating of the ice core is discussed extensively in Fisher et al. (1983), Fisher and Koerner (1988) and is accurate to $\pm$ 10%. The theoretical time scale was adjusted using volcanic statigraphy. Dates were assigned using known historical records or the dates given by the Dye 3 ice core (Fisher and Koerner, 1994).

3. Analysis

In this section we (a) obtain the ground temperature history from geothermal data, (b) filter the oxygen isotope data to make it comparable to the GTH from geothermal data, (c) find a relation between the filtered oxygen isotope data and the GTH and express the oxygen isotope data in terms of ground temperature variations, and finally, (d) reconstruct a synthetic subsurface temperature profile from the calibrated oxygen data. The theoretical framework is given in the appendix.

3.1. GTH from geothermal data

Considering that the available $\delta^{18}O$ isotope time series from the Agassiz ice cap consists of 25-year averages, we have chosen a model ground temperature history comprising eighty 25-years step temperature changes extending to 2000 years before measurements; older variations would not be recorded in detail in the upper 600 m of the Earth' crust.

The GTH from the Neil well was obtained by inverting the full temperature–depth profile, using SVD with the singular value cutoff ratio set at 0.025. The Bullard plot (Bullard, 1939) is evaluated internally by the inversion procedure (Eqs. 2 and 3 in the Appendix) to compensate for the thermal conductivity changes as measured in rock samples. Fig. 2b shows the subsurface temperature perturbation deter-

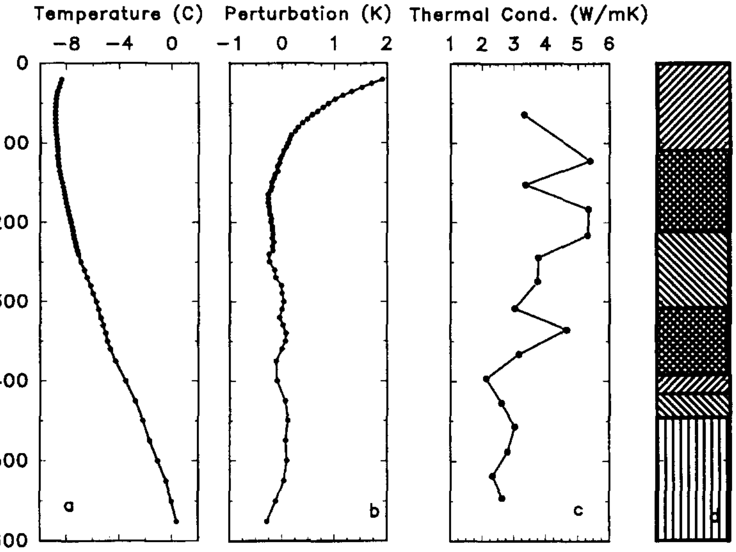

Fig. 2. a. Temperature–depth profile measured at the Neil site in 1991. b. Temperature anomaly assumed caused by ground temperature changes at the surface. Thermal conductivity variations (c) have been taken into account to determine this anomaly (see text). d. Lithology at Neil site. Layers from top to bottom are: shale, shale and sandstone, siltstone, sands and siltstone, shale, siltstone, sandstone and shale.

mined by the inversion. The long term surface temperature (−10.65°C) and heat flow density (62.7 mW/m^2) were simultaneously found from the inversion. Fig. 4 shows the last 1000 years of the GTH obtained for the Neil well temperature log. The present ground temperature is about −8°C (Fig. 2a), about 2.6 K higher than the long term mean or reference temperature. The temperature anomaly shown in Fig. 2b is proportional to the heat absorbed or released by the ground and the time evolution of this heat imbalance is given by the ground temperature history. The heat absorbed by the ground in the last 100 years at the Neil site is of the order of 0.1 W/m^2, smaller than reported for Awuna (0.16 W/m^2, Lachenbruchet al., 1988) in Alaska. Such heat fluxes are very small and undetectable by direct measurement.

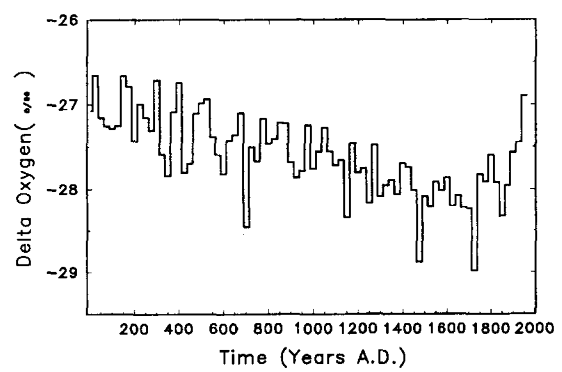

Fig. 3. Oxygen isotope data (25 year averages) from the Agassiz ice cap ice core for the last 2000 years (Fisher et al., 1983).

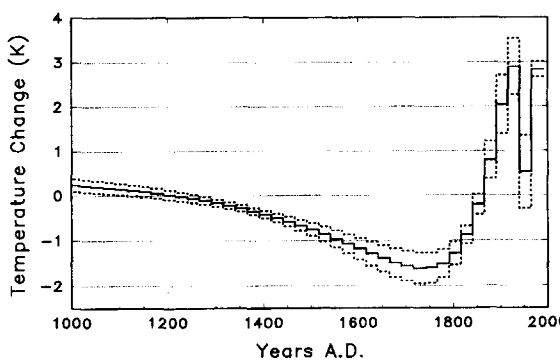

Fig. 4. Ground temperature history (solid line) derived through inversion of the temperature–depth data at the Neil site. The model consists of eighty 25-year step temperature changes; only the last 1000 years are shown. Dashed lines represent the standard error (SE) of the estimated model parameters for an assumed 0.10 K data standard deviation. These SE are a measure of the stability of the GTH to noise.

3.2. Filtering the oxygen isotope time series

A direct comparison of the Neil GTH with Agassiz $\delta^{18}O$ data is not quantitatively possible since the records are not of the same resolution. In particular, the GTH model parameters as determined by the inversion of geothermal data are averaged over a time window which increases in length the further the event is in the past (see appendix). Simply filtering the high resolution oxygen isotope data series using moving averages or polynomial fits is too arbitrary since these processes do not have a physical justification.

It is thus necessary to filter the oxygen series through the same physical averaging process as heat diffusion filters the details of the GTH. That is, the oxygen isotope series must be degraded to match the resolution of the GTH. This procedure can be accomplished simply by multiplying the 25-year average oxygen isotope series by the model resolution matrix from the geothermal data inversion. Before multiplying the oxygen series by the resolution matrix, the oxygen isotope series was transformed as a series of departures from −27.64‰ (after Taylor, 1991). The model resolution matrix, as discussed in the Appendix, relates the estimated parameters to the true parameters obtained in the inversion, in a way that incorporates the physics of heat diffusion and the geometry of the problem. A multiplication of the 25-year oxygen series by the resolution matrix is equivalent to inverting a subsurface profile generated from the oxygen series, without the need of specifying the relationship between oxygen data and ground temperatures. This approach is general enough to be applied to other proxy climatic indicators, tree-ring widths for example (Beltrami et al., 1995). Fig. 5a shows the full model resolution matrix; the rapid loss of resolution with time can be readily observed. Fig. 5b shows several slices of the model resolution matrix at the given times. The height of the peaks represents the resolution of the model parameters at these times and the width of each peak yields an estimate of the spread of the resolution. An event can only be fully resolved if its duration is at least 60% of the time of occurrence (Beltrami and Mareschal, 1995).

The filtered or "diffused" $\delta^{18}O$ series (Fig. 6) can now be directly compared with the GTH derived from geothermal data. Only the last 1000 years of the filtered $\delta^{18}O$ time series and the original 25-years averages are shown.

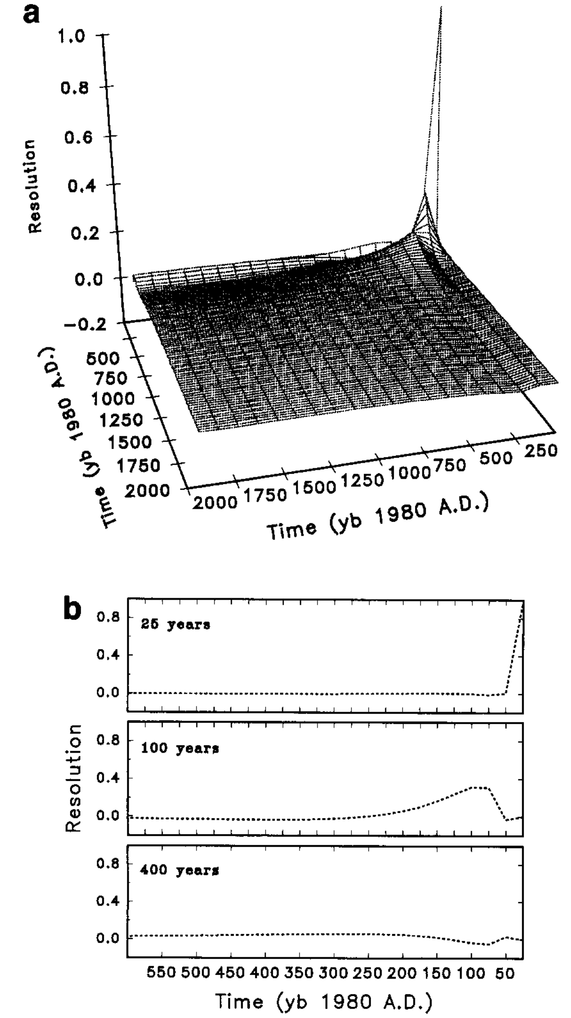

Fig. 5. a. Model resolution matrix **R** (Eq. A-8) for the GTH model used to obtain Fig 4. b. Slices of the model resolution matrix at 25, 100 and 400 years showing that the model resolution decreases rapidly in time.

The times series in Fig. 4 and Fig. 6 reach their maximum values this century, have minima around 1800 A.D., and return to values just less than reference value at about 1200 A.D. The first dip in the two series at approximately 1960 A.D. is the result of oscillations in the inversion procedure arising from the fact that the first time step was set based on

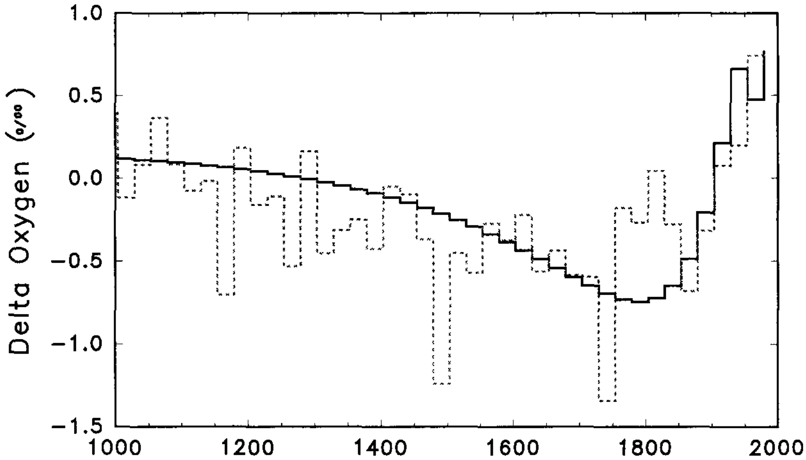

Fig. 6. Filtered oxygen isotope data (solid line) obtained through multiplication of the oxygen data (dashed line) by the model resolution matrix **R** determined from inversion of the geothermal data.

the resolution of the available delta oxygen series. Since the first few meters ofthe temperature log are the noisiest due the residues of the short-term temperature variations (< 10 years), the first and second model parameters are affected. In principle, this oscillation can be easily eliminated by increasing the size of the first model step.

3.3. Calibration of oxygen isotope data

The second part in this procedure involves the direct comparison of the GTH with the filtered oxygen data. In Fig. 7, the GTH from geothermal data and the filtered oxygen isotope series (Fig. 6) have been plotted against each other for succesive 25-year periods in the past. The first two data point have been deleted for the reasons explained above. The relation between these quantities appears to be regular and we assume it is linear and given by:

$$\Delta T_g = 2.38\,\delta^{18}O + 0.046$$

$$\delta^{18}O = 0.42\,\Delta T_g - 0.019 \qquad (1)$$

where ΔT_g is the 25-year temperature change from the long term mean and $\delta^{18}O$ is the 25-year average delta oxygen from the filtered series of departures. The delta oxygen data have now been calibrated against ground temperature changes.

3.4. Reconstruction of subsurface temperature profile

We use Eq. 1 to transform the 25-year values of the 2000-year δ^{18}O series into equivalent ground temperature changes. This yields a reconstructed ground temperature history from the oxygen data with significantly higher resolution than that obtained from geothermal data alone (HR-GTH, Fig. 8).

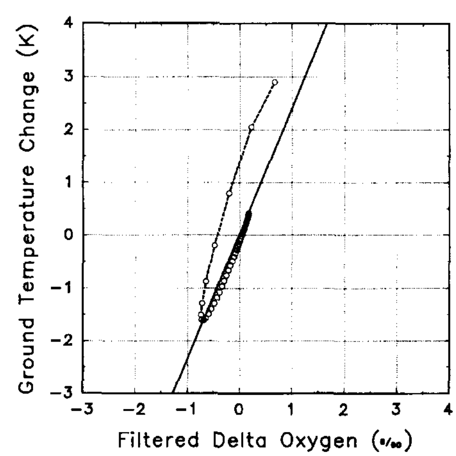

Fig. 7. Relation between ground surface temperature changes (GTH) and filtered oxygen isotope data. A linear least squares fit was carried out through all the data shown.

A fundamental requirement for the acceptance or rejection of a HR-GTH is whether it satisfactorily explains the observed subsurface thermal regime. For the moment we assume that the climate and environmental conditions at both the Agassiz ice cap and at the Neil well site, separated by some 180 km, has been the same for the last 2000 years (see discussion in Taylor, 1991). The agreement of the model prediction and measured data can be verified by using the HR-GTH series as a forcing function at the Earth's surface and solving the forward problem. The synthetic subsurface profile generated in this fashion depends as well on the background temperature before the start of this thermal history. In the case of the GTH from geothermal data, this background is determined by the "undisturbed" or reference geothermal heat flow density at depths which are not significantly affected by recent ground surface temperature changes. Since the reference delta oxygen was set arbitrarily to today's value, we can invert the HR-GTH subsurface profile generated from the oxygen series to identify the background temperature that can best explain the observed anomaly profile. This consists of a D.C. shift in the synthetic profile. A similar approach was used successfully by Lachenbruch et al. (1988) and Chisholm and Chapman (1992) when obtaining pre-observational means for meteorological data in Alaska and Utah respectively. Once the background has been determined the high resolution temperature reconstruction can be corrected and expressed in terms of departures from a long term mean ground temperature.

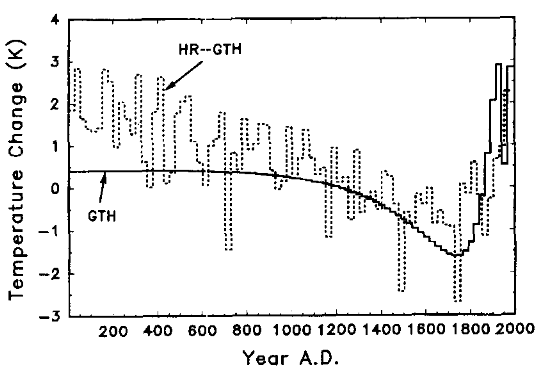

Fig. 8. High resolution ground temperature history (HR-GTH) reconstructed from oxygen isotope data (dashed line). Solid line represents the GTH from geothermal data only (Fig. 4).

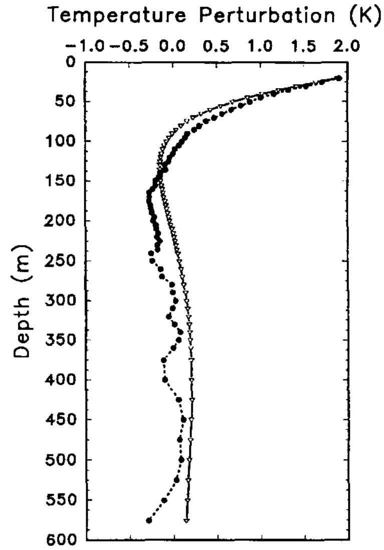

Fig. 9. Subsurface temperature anomalies. Circles, the estimated subsurface temperature perturbation from measurements (Fig. 2b); triangles, the anomaly obtained when the calibrated oxygen series is used as a forcing function at the surface.

Fig. 8 compares the GTH from geothermal data alone and the HR-GTH obtained from the combination of geothermal and oxygen isotope data. The subsurface temperature profile generated from the HR-GTH appears similar to the observed temperature anomaly (Fig. 9). The "bumps" in the data are due to small scale thermal structure variability which

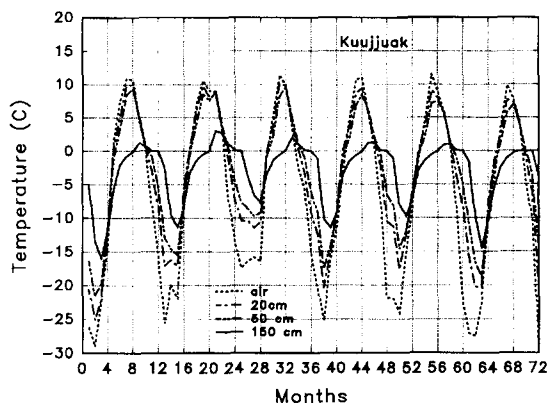

Fig. 10. Time series (72 months) of air and near surface soil temperatures for Kuujjuak for part of the existing record. The amplitude variation and phase shifts as a function of depth are apparent.

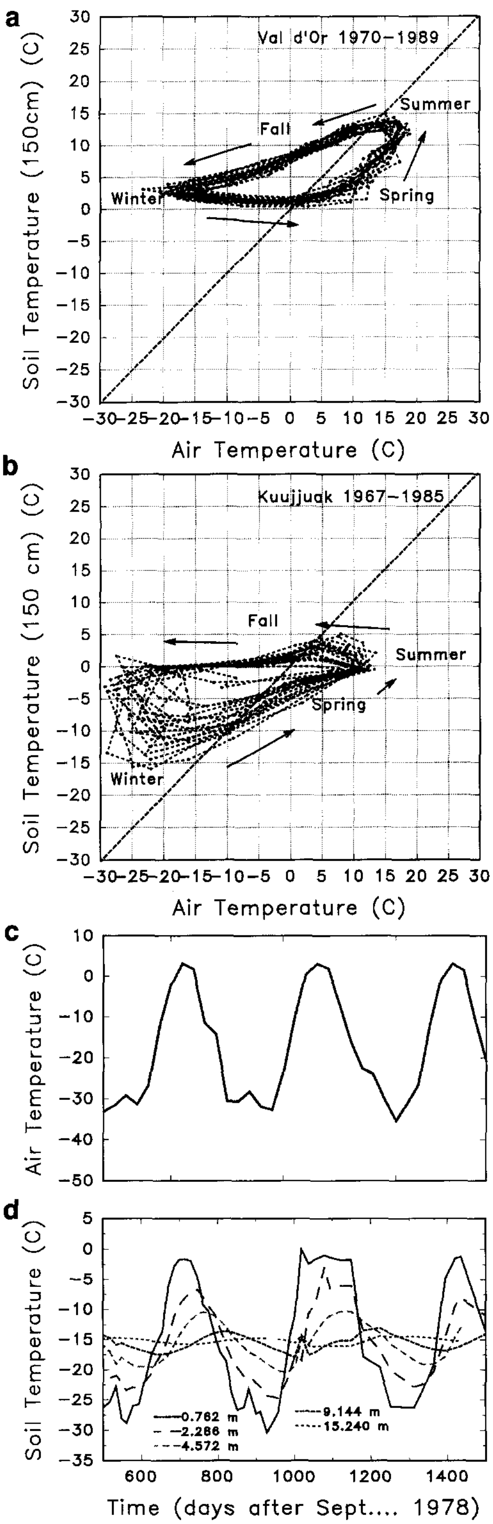

Fig. 11. "Phase space" plots for air and soil monthly averages temperature record at (a) Val d'Or, (b) Kuujjuak. (c) Monthly mean air temperatures from January 1980 to October 1982 at Alert (data from Environment Canada). (d) Soil temperatures measured in a borehole at Alert for the same period.

cannot be corrected for with only a few thermal conductivity measurements; similar structures are common and have been observed at other locations (Harris and Chapman, 1995; Beltrami and Mareschal, 1995).

4. Discussion

Ground temperatures integrate the effects of air temperatures, snow cover, and active layer processes at these latitudes, and they are not necessarily a direct reflection of air temperature. Fig. 10 shows 72 months of the record of air and soil temperatures at several depths, measured at Kuujjuak (Québec, 58°06′ N, 68°25′ W) (data from Environment Canada). The well known decrease in amplitude and shift in phase with respect to air temperatures are clearly seen (Geiger, 1965; Smith, 1975; Smith and Riseborough, 1983).

In lower latitudes ground temperatures may never reach the freezing point (at least during the period of measurements) because of snow cover and the relation between air and soil temperatures can be instructive. Fig. 11a shows the relation between monthly mean air temperatures and soil temperatures at a depth of 150 cm measured at Val d'Or, Québec (48°04′ N, 77°47′ W), over 19 years. This figure can be interpreted as the interception of two quasi-sinusoidal variations in time with different amplitudes and phase (phase-space plot) arising from the heat capacity of the ground; these are analogous to the Lissajous figures of electrical engineering. The ellipsoids appear somewhat deformed. During the summer, the measurements are taken at a depth of 150 cm, but in winter the true depth of measurement is the summer depth plus the snow cover equivalent in terms of ground depth. Winter measurements are related to effective ground depth by the thermal diffusivity of the snow cover. Thus, the figures shown are a composite of a "summer ellipsoid" and a "winter ellipsoid" whose phase and amplitude change with snow cover. The regularity of this figure implies a direct relation between air temperature and ground temperature in the long-term as long as snow cover variations are small. In a sense, the phase-space plot describes a "cloud of probability" where trajectories in air-soil temperature space are to be found. Examination of air and soil temperature records at other locations in Canada confirms this regular behaviour. This type of analysis of subsurface soil to soil temperatures at different depths permits the identification of conduction and non-conduction dominated heat transfer regimes (Beltrami, 1995, manuscript in prep.).

On the other hand, in Fig. 11b, we show a phase-space plot (150 cm) at Kuujjuak. The effects of the active layer processes are apparent with the soil temperature at 150 cm remaining close to the freezing point for one or two months in the Fall. This is due to the freezing of the ground above 150 cm and its subsequent latent heat release. Furthermore, at the peak of the summer (seasons proceed counterclockwise), the soil temperature increases rapidly after thawing of the upper layer of soil. The monthly averages used to create these figures do not have the resolution to observe finer details. For this station, small changes in snow cover, or variability of the air temperature can be a large source of spread and thus make the phase–space plots shown here very irregular.

Thus Fig. 11 a, b illustrates the latitudinal effects of snow cover and active layer processes on ground temperatures. Unfortunately, there are no complete (i.e. air and soil temperature data) meteorological records in the Agassiz-Neil area and it is difficult to evaluate the effects of melting and freezing of the upper soil layer on ground temperature and temperature–depth profile, at the borehole site. However, soil temperature measurements taken at an Alert borehole for 12 years at irregular time intervals (Taylor, unpublished data) indicate that the active layer at the borehole site is less than 0.5 m. Fig. 11c, d, shows part of these ground temperature data and monthly mean air temperature records for the same time period (January 1980–October 1982); it is not possible to generate a "phase space" diagram for these records because of the unequal soil temperatures sampling intervals.

5. Conclusions

The coefficient between delta oxygen ratios and *air temperature* change varies considerably (Grootes and Steig, 1992). Cuffey et al. (1992) obtained avalue of 0.75‰ K^{-1} for Greenland, subsequently this value was corrected to 0.5‰ K^{-1} (Cuffey et al., 1994) and Fisher et al. (1983) used the value 0.6‰ K^{-1} for the Agassiz data. It is important to make clear that the relation in the present work, 0.42‰ K^{-1}, is for delta oxygen ratios and *ground temperature variations*; it should not be readily applied to air temperatures.

Since we have reproduced the subsurface thermal profile at the Neil well with oxygen isotope data from the Agassiz site (Fig. 9), we suggest that the oxygen data does represents long-term climatic variations in the Arctic. However, there are differences that can be attributed to the different characters of the records and differences in location. The ice cap and the Neil borehole are separated by a distance of 180 km and they are also at different elevations (1700 m and 497 m, respectively). Ground temperature responds to a large number of climatic variables with air temperature, snow cover and active layer processes being the dominant ones. The fact that the two profiles in Fig. 9 are similar implies that *variations* of snow cover have been small and active layer processes have not been significant at the site of the borehole for the period studied here. Hence, oxygen isotope data are a reasonable indicator of regional long-term temperature change.

Acknowledgements

H.B. acknowledges support from a postdoctoral fellowship from the Natural Sciences and Engineering Research Council of Canada (NSERC) and O. Jensen (McGill). We thank D. Fisher and R. Alley for comments on an early version of this paper, and D.S. Chapman and Friends of Lord Kelvin for discussions. We are grateful to A. Lachenbruch and G. Vasseur for constructive reviews which helped to improve this communication. GSC contribution number 34594.

Appendix A. Theoretical framework

For an homogeneous, isotropic, source-free half space, the temperature perturbation due to a time varying ground surface temperature is a solution of the heat diffusion equation in one dimension with initial and boundary conditions (Carslaw and Jaeger, 1959):

$$\kappa \frac{\partial^2 T}{\partial z^2} = \frac{\partial T}{\partial t}, \tag{a1}$$

where κ is the thermal diffusivity of the rock, z is depth (positive downwards), and t is the time. The use of the one-dimensional equation is valid if long term surface temperature changes are constant across an area much larger than the depth to which they penetrate.

The temperature at depth z, $T(z)$, is the superposition of the equilibrium temperature and of $T_t(z)$, the temperature perturbation arising from the time varying surface temperature. i.e.

$$T(z) = T_o + q_o R(z) = T_t(z), \tag{a2}$$

where T_0 is the long term ground temperature, q_o is the quasi-equilibrium surface heat flow density, assumed to exist in the deepest parts of the temperature log, least effected by recent ground temperature changes, $R(z)$ is the thermal resistance from the surface to the depth z (Bullard, 1939):

$$R(z) = \int_o^z \frac{dz'}{K(z')} \tag{a3}$$

where $K(z)$ is the thermal conductivity measured in core samples and/or estimated from the lithology.

For an instantaneous change in ground surface temperature T at time t before present, the subsurface temperature perturbation is given by (Carslaw and Jaeger, 1959):

$$T_t(z) = T \operatorname{erfc} \frac{z}{2\sqrt{\kappa t}}, \tag{a4}$$

where erfc is the complementary error function.

Since short period variations are attenuated rapidly with depth (e.g. Carslaw and Jaeger, 1959), the surface temperature history can be approximated by the average surface temperature over a series of time intervals that are often assumed of equal duration Δ:

$$T_0(t) = T_k \quad (k-1)\Delta \leq t < k\Delta \tag{a5}$$

and $k = 1, \ldots K$. The assumption of equal duration is not necessary but has been made only for the sake of simplicity.

Eq. A-2 can then be written as:

$$\Theta_j = A_{jl} X_l \tag{a6}$$

where Θ_j are the J values of temperature measured at depth z_j, corrected for heat production between the surface and that depth if necessary. X_l is a vector containing the parameters, i.e. the equilibrium temperature, heat flow and the averaged past surface temperatures so that $\mathbf{X} = \{T_0, q_0, T_1, \ldots, T_K\}$. A_{jl} is a matrix containing 1's in the first row, the thermal resistance to depth z_j, $R(z_j)$, in the second row, and, in the K following rows, the J elements formed by evaluating the difference between complementary error functions at depth z_j and times t_{k-1} and t_k:

$$A_{jk+2} = \operatorname{erf}c\left\{\frac{z_j}{2\sqrt{\kappa t_k}}\right\} - \operatorname{erf}c\left\{\frac{z_j}{2\sqrt{\kappa t_k - 1}}\right\} \tag{a7}$$

This yields an overdetermined system of linear equations. Mareschal and Beltrami (1992), Harris and Chapman (1995) and Beltrami and Mareschal (1995) have used the singular value decomposition (SVD) method to obtain a generalized solution to this system (Lanczos, 1961).

The model resolution matrix **R** is defined as:

$$\boldsymbol{R} = \boldsymbol{V}\boldsymbol{V}^T \tag{a8}$$

where only the model space eigenvectors, **V** (from SVD), corresponding to non-zero singular values are retained. The matrix **R** depends only on the data kernel of **A**, i.e. the experimental geometry and the assumptions applied to the model. They are independent of the actual values of the data. The matrix **R** relates the parameters of a model to the parameters that would be obtained by inversion of the corresponding data (e.g. Menke, 1989) $\mathbf{T}^{est} = \mathbf{R}\mathbf{T}^{true}$. The model parameters are perfectly resolved if **R** is an identity matrix; if **R** is not an identity matrix, the model parameters are given as averages of the true model parameters. We note here that to compare a GTH obtained by inversion of geothermal data with high resolution climatic indicators is thus necessary to multiply the climatic time series by the model resolution matrix in order to compare values averaged by the same process.

If all the vectors in **V** were retained, the model resolution matrix would be the identity matrix. The resolution is limited because the rank of the system is less than the dimension of model space; it is further reduced by the elimination of the small singular values (Beltrami and Mareschal, 1992). The inclusion of more singular values improves the resolution, but it also increases the variance of the estimated model parameters because of the amplification of noise (Mareschal and Beltrami, 1992). This is the common trade off between resolution and stability of a solution. The choice of one at the expense of the other depends on the quality of the data as well as on the character of the problem (Parker, 1994).

References

Beltrami, H., Jessop, A. and Mareschal, J.C., 1992. Ground temperature histories in eastern and central Canada from geothermal measurements. Palaeogeogr. Palaeoclimatol. Palaeoecol. (Global Planet. Change Sect.), 98: 167–184.

Beltrami, H. and Chapman, D.S., 1994. Drilling for a past climate. New Sci., 142: 36–40.

Beltrami, H. and Mareschal, J.C., 1991. Recent warming in eastern Canada: Evidence from geothermal measurements. Geophys. Res. Lett., 18: 605–608.

Beltrami, H. and Mareschal, J.C., 1992. Ground temperature histories for central and eastern Canada from geothermal measurements: Little Ice Age signature. Geophys. Res. Lett., 19: 698–692.

Beltrami, H. and Mareschal, J.C., 1993. Determination of past climate change from geothermal data: Regional ground temperature histories, correlation with atmospheric CO_2 and comparison with proxy data. Terra Nova, 5: 21–28.

Beltrami, H. and Mareschal, J.C., 1995. Resolution of ground temperature histories inverted from borehole temperature data. Global Planet. Change, 11: 57–70.

Beltrami, H., Chapman, D.S., Archambault, S. and Bergeron, Y., 1995. Reconstruction of high resolution ground temperature histories combining dendrochronological and geothermal data. In press.

Bradley, R.S., 1985. Quaternary Paleoclimatology: Methods of Paleoclimatic Reconstruction. Allen and Unwin, Boston, 472 pp.

Bullard, E.C., 1939. Heat Flow in South Africa. Proc. R. Soc. London A, 173: 474–502.

Carslaw, H.S. and Jaeger, J.C., 1959. Conduction of Heat in Solids. Oxford Univ. Press, 2nd ed., 510 pp.

Charles, C.D., Rind, D., Jouzel, J., Koster, R.D. and Fairbanks, R.G., 1994. Glacial–interglacial changes in moisture sources for Greenland: Influences on the ice core record of climate. Science, 263: 508–511.

Chisholm, T.J. and Chapman, D.S., 1992. Climate change inferred from analysis of borehole temperatures: an example from western Utah, J. Geophys. Res., 97: 14,155–14,176.

Clow, G., 1992. Temporal resolution of surface-temperature histories inferred from borehole temperature measurements. Palaeogeogr. Palaeoclimatol. Palaeoecol. (Global Planet. Change Sect.), 98: 81–86.

Cuffey, K.M., Alley, R.B., Grootes, P.M. and Anandakrishnan, S., 1992. Towards using borehole temperatures to calibrate an isotopic paleothermometer in central Greenland. Palaeogeogr. Palaeoclimatol. Palaeoecol. (Global Planet. Change Sect.), 98: 265–268.

Cuffey, K.M., Alley, R.B., Grootes, P.M., Bolzan, J.M. and Anandakrishnan, S., 1994. Calibration of the $\delta^{18}O$ isotopic paleothermometer in central Greenland using borehole temperatures. J. Glaciol., 40: 341–349.

Fisher, D.A. and Koerner, R.M., 1988. The effects of wind on $\delta^{18}O$ and accumulation give an inferred record of seasonal δ amplitude from the Agassiz Ice Cap, Ellesmere Island, Canada. Ann. Glaciol., 10: 34–37.

Fisher, D.A., Koerner, R.M., Paterson, W.S.B., Dansgaard, W., Gundestrup, N. and Reeh, N., 1983. Effect of wind scouring on climatic records from ice-core oxygen isotope profiles. Nature, 301: 205–209.

Fisher, D.A. and Koerner, R.M., 1994. Signal and noise in four ice-core records from the Agassiz Ice Cap, Ellesmere Island, Canada: details of the last millennium for stable isotopes, melt and solid conductivity. Holocene, 4: 113–120.

Geiger, R., 1965. The Climate Near the Ground. Harvard Univ. Press, Cambridge, MA, 611 pp.

Grootes, P.M. and Steig, E.J., 1992. Uncertainties in the isotope-temperature relationship in ice cores (abstract). EOS (Suppl. April 7, 1992), p. 107.

Harris, R.N. and Chapman, D.S., 1995. Climate change on the Colorado Plateau of eastern Utah inferred from borehole temperatures. J. Geophys. Res., in press.

Jessop, A.M., 1990. Thermal Geophysics. Elsevier, Amsterdam, 306 pp.

Lachenbruch, A.H. and Marshall, B.V., 1986. Changing climate: geothermal evidence from permafrost in the Alaskan Arctic. Science, 234: 689–696.

Lachenbruch, A.H., Cladouhos, T.T. and Saltus, R.W., 1988. Permafrost temperature and the changing climate. Proc. 5th Int. Conf. Permafrost, Trondheim, August, 1988.

Lanczos, C., 1961. Linear Differential Operators. Van Nostrand, New York, 564 pp.

Mareschal, J.C. and Beltrami, H., 1992. Evidence for recent warming from perturbed geothermal gradients: examples from eastern Canada. Clim. Dyn., 6: 135–143.

Menke, W., 1989. Geophysical Data Analysis: Discrete Inverse Theory (Int. Geophys. Ser., 45). Academic Press, San Diego, 289 pp.

Parker, R.L., 1994. Geophysical Inverse Theory. Princeton Univ. Press, Princeton, NJ, 386 pp..

Pollack, H.N. and Chapman, D.S., 1993. Underground records of changing climate. Sci. Am., 268: 44–50.

Sass, J.H., Lachenbruch, A.H. and Munroe, R.J., 1971. Thermal conductivity of rocks from measurements on fragments and its application to heat flow determinations, J. Geophys. Res., 76: 3391–3401.

Shen, P.Y. and Beck, A.E., 1992. Paleoclimate change and heat flow density inferred from borehole temperature data in the Superior Province of the Canadian Shield. Palaeogeogr. Palaeoclimatol. Palaeoecol. (Global Planet. Change Sect.), 98: 143–165.

Smith, M.W., 1975. Microclimatic influences on ground temperatures and permafrost distribution, Mackenzie Delta, Northwest Territories. Can. J. Earth Sci., 12: 1421–1438.

Smith, M.W. and Riseborough, D.W., 1983. Permafrost sensitivity to climate change. Proc. Permafrost, 4th Int. Conf. Natl. Acad. Press, Washington, DC, pp. 1178–1183.

Taylor, A.E., Burgess, M., Judge, A.S. and Allen, V.S., 1982. Canadian Geothermal Data Collection—Northern Wells, 1981 (Geothermal Ser., 13). Earth Physics Branch, EMR Canada, 153 pp.

Taylor, A.E., 1991. Holocene paleoenvironmental reconstruction from deep ground temperatures: a comparison with paleoclimate derived from the $\delta^{18}O$ record in an ice core from the Agassiz Ice Cap. Canadian Arctic Archipelago. J. Glaciol., 37: 209–219.

Thompson, L.G., Mosley-Thompson, E., Dansgaard, W. and Grootes, P.M., 1986. The Little Ice Age as recorded in the stratigraphy of the tropical Quelccaya Ice Cap. Science, 234: 361–364.

Vasseur, G. and Mareschal, J.C., 1993. Les Forages: Une fenêtre sur les Climats Passées. Recherche, 258: 1076–1082.

Wang, K., Lewis, T.J. and Jessop, A.M., 1992. Climatic changes in central and eastern Canada inferred from deep borehole temperature data. Palaeogeogr. Palaeoclimatol. Palaeoecol. (Global Planet. Change Sect.), 98: 129–141.